CHAPTER 2

SPECTRA AND THRESHOLDS OF LASING OF THE MODES OF CIRCULAR RESONATORS

In this Chapter, considered are the 2-D models of the circular-disk uniformly and partially active open dielectric resonators. Natural lasing electromagnetic modes of these resonators are sought as non-attenuating in time electromagnetic fields able to exist without external sources. They have to satisfy the boundary-value problems for the Helmholtz equation with continuity conditions on the boundaries of partial domains, condition of local finiteness of energy, and the radiation condition at infinity. The presence of the active region is modeled with the aid of negative-loss imaginary part of refractive index in the corresponding domain. Research is aimed at the frequencies and thresholds of lasing in the simplest form of such resonators and also the ways of lowering the thresholds.

2.1. Reduction of dimensionality of boundary-value problem

Consider a vector 3-D problem about the natural electromagnetic fields (modes) of a dielectric open resonator having the shape of flat disk (not necessarily circular) bounded by two identical flat-parallel surfaces with the distance *d* between them and a side surface, as depicted in Fig. 2.1. Introduce the coordinate systems as shown in the figure: Cartesian (x, y, z), cylindrical (r, φ, z) and spherical (R, φ, θ). Assume that the relative dielectric permittivity ε of the resonator material can be complex-valued. At first, assume that the resonator is passive, so that $\mathrm{Im}\,\varepsilon \geq 0$. The problem implies finding those values (eigenvalues) of the frequency or, what is more convenient, the wavenumber $k = \omega / c$ (frequency normalized to *c*), which generate non-zero electromagnetic field functions $\{\dot{\vec{E}}, \dot{\vec{H}}\}$ in the presence of resonator.

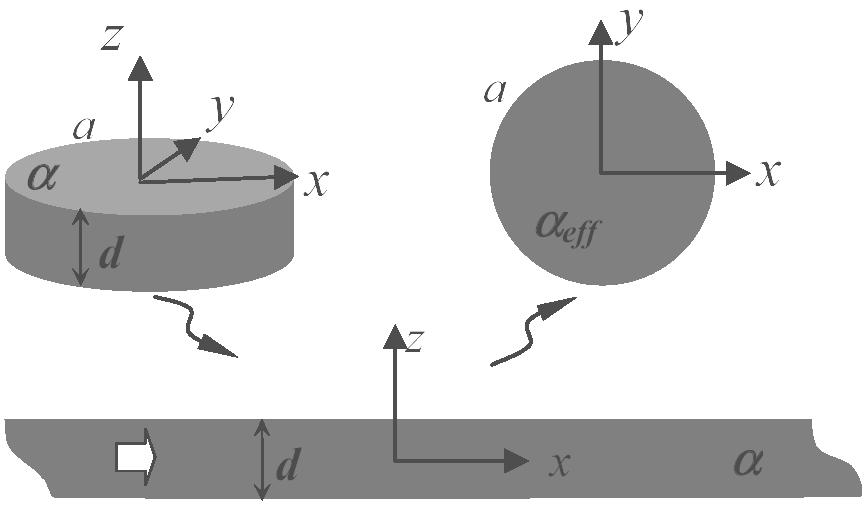

Fig. 2.1 Three-dimensional thin-disk dielectric resonator and related configurations of reduced dimensionality: flat-parallel slab and two-dimensional resonator in the *XY* plane.

These fields must be solutions of the time-harmonic (: $e^{-i\omega t}$) Maxwell equations off the whole boundary of the resonator, *S*

$$curl\ \dot{E} = ikZ_0\,\dot{H}, \quad curl\ \dot{H} = -ik\alpha^2 Z_0^{-1}\dot{E}, \tag{2.1}$$

where $Z_0 = (\mu_0/\varepsilon_0)^{1/2}$ is the free-space impedance, $\alpha = \sqrt{\varepsilon}$ is the piece-constant complex refractive index, equal to 1 outside of the resonator; we will also assume that $\mathrm{sign}(\mathrm{Im}\,\alpha) = \mathrm{sign}(\mathrm{Im}\,\varepsilon)$. Besides, on the surface *S* the following conditions of continuity must be satisfied for the tangential field components:

$$\dot{E}^{-}_{\tan} = \dot{E}^{+}_{\tan}, \quad \dot{H}^{-}_{\tan} = \dot{H}^{+}_{\tan}, \tag{2.2}$$

where the upper index "$\pm$" indicates to the limit values of the functions from inside and from outside of the disk, respectively, and the lower index «*tan*» denotes the field components tangential to the surface *S*. Further, the electromagnetic field energy

must be locally finite to exclude the source-type field singularities,

$$\int_V [\alpha^2 E^2(\vec{R}) + H^2(\vec{R})] d\vec{R} < \infty, \quad V \subset (r, \varphi, z), \tag{2.3}$$

Finally, it is necessary to include into the formulation certain condition characterizing the field behavior at infinity, $R \to \infty$. This condition plays very important role and, eventually, determines the location of the eigenfrequencies. For example, if interested in the real-valued frequencies, $k = \mathrm{Re}\, k$, then one should impose the Silver-Muller radiation condition [107]:

$$\lim_{R\to\infty} \left\{ \vec{E}(\vec{R}) - Z_0 \vec{H}(\vec{R}) \times \vec{R} / R \right\} = 0, \tag{2.4}$$

which serves as vector 3-D analog of the Sommerfeld condition used in the theory of scalar waves satisfying the Helmholtz equation. The condition (2.4) provides for the field to behave as a spherical wave and, additionally, eliminates the radial field components at infinity. It can be equivalently written as a set of asymptotic requests,

$$\begin{aligned} & e^{-ikR} \{E_R, H_R\} \sim 0, \; E_\varphi = Z_0 H_\theta \sim \frac{e^{ikR}}{R} \Phi_1(\varphi, \theta), \\ & E_\theta = -Z_0 H_\varphi \sim \frac{e^{ikR}}{R} \Phi_2(\varphi, \theta), \qquad R \to \infty \end{aligned} \tag{2.5}$$

In the scattering problems, the conditions (2.1)–(2.4) are imposed at the scattered field and guarantee the uniqueness of solutions provided that the frequency is not an eigenvalue of the problem. Assume now that some frequency k is an eigenvalue and so generates non-zero eigenfield $\{\vec{E}, \vec{H}\}$. Then the Poynting Theorem applied to the function $\{\vec{E}, \vec{H}\}$ and its complex-conjugate leads to the conclusion that independently of the geometry of open resonator the real-valued eigenfrequencies cannot exist.

Thus, to stay adequate to the physical situation, one must admit the complex values of k. In this case the condition (2.5) is still applicable because it is valid for arbitrary complex k. Further, the same Poynting Theorem leads to the conclusion that for a passive resonator all possible eigenvalues of *k* can be located only in the lower halfplane of k-plane. It means that every eigenvalue may have only strictly negative imaginary part, $\mathrm{Im}\, k < 0$ (for the selected time dependence; if it were selected as $e^{i\omega t}$ then the imaginary part of k may be only strictly positive). Therefore these eigenvalues are in fact the generalized eigenvalues (a.k.a. scattering frequencies); they generate generalized vector-functions $\{\vec{E}, \vec{H}\}$, whose components diverge at infinity as $O(e^{-\mathrm{Im}\, kR} / R)$ in accordance to (2.5). However, if in some part of the open resonator $\mathrm{Im}\, \varepsilon < 0$ (i.e. its material displays active behavior under pumping) then purely real eigenvalues of *k* become allowed.

Three-dimensional problem (2.1) – (2.4) is difficult for the investigation. However for the thin disk-like resonators it can be approximately reduced to the 2-D problem for the field function in the median plane of the resonator. Such a reduction of dimensionality is called the method of effective refractive index (see [60], [63], [65], [66], [142]-[146]). In fact, this method is based on the assumption that the electromagnetic field in the whole space can be presented as a product of two functions of independent variables *z* and $\vec{r} = (r, \varphi)$; for instance,

$$E_z(\vec{R}) = V_E(z) U_E(r, \varphi), \quad H_z(\vec{R}) = V_H(z) U_H(r, \varphi) \tag{2.6}$$

In reality, this assumption is not correct as the mentioned variables separate neither in the boundary conditions on the disk surface nor in the radiation condition at $R \to \infty$. However the assumption (2.6) leads to two independent differential equations for the functions of the vertical variable *z* and of the in-plane variables r, φ,

$$\left[d^2 / dz^2 + k^2 \alpha^2 - k^2 \left(\alpha_{eff}^{E,H} \right)^2 \right] V_{E,H}(z) = 0, \tag{2.7}$$

where α equals 1 off the interval $|z|<d/2$ (see Fig. 2.1), and

$$\left[\frac{1}{r}\frac{\partial}{\partial r}\left(r\frac{\partial}{\partial r}\right)+\frac{1}{r^2}\frac{\partial^2}{\partial\varphi^2}+k^2\alpha_{eff}^2\right]U_{E,H}(r,\varphi)=0, \qquad (2.8)$$

where the coefficient $\alpha_{eff}=\alpha_{eff}^{H,E}$ equals 1 off the resonator. Thus, the value $k^2\alpha_{eff}^2$ plays role of the separation constant in the separation of variables. The boundary conditions for the introduced partial functions depend on the polarization. Although, strictly speaking, in the presence of a 3-D resonator the field has all six non-zero components, the reduction of dimensionality leads to two independent types of field functions: E-polarized $(0,0,E_z,H_r,H_\varphi,0)$ and H-polarized $(E_r,E_\varphi,0,0,0,H_z)$. For the function of the variable z it is requested that

$$\begin{aligned} &V_{H,E}(\pm d/2\,\mathrm{m}0)=V_{H,E}(\pm d/2\pm 0),\\ &\left.\frac{dV_{H,E}}{dz}\right|_{z=\pm d/2\mathrm{m}0}=\beta^{H,E}\left.\frac{dV_{H,E}}{dz}\right|_{z=\pm d/2\pm 0}, \end{aligned} \qquad (2.9)$$

where $\beta^H=\alpha^{-2}$ and $\beta^E=1$.

Still something should be done with the other conditions. Unfortunately, there is no any formal way to obtain 1-D radiation condition from the 3-D condition (2.5). Nevertheless, for the sake of keeping the physical meaning intact, i.e. to reproduce the field behavior as either decaying or propagating off the disk plane (no incoming waves), one should demand that the following condition is satisfied:

$$V_{E,H}(z)\sim e^{ik(1-\alpha_{eff}^2)^{1/2}|z|}, \quad z\to\pm\infty, \qquad (2.10)$$

Equations (2.7), (2.9) and (2.10), for $\beta^H=\alpha^{-2}$ и $\beta^E=1$, form two well known

1-D eigenvalue problems for the parameters α_{eff}^{H} and α_{eff}^{E}, respectively, which are the normalized by *k* propagation constants of the TE and TM waves, respectively, traveling along the infinite dielectric slab of the thickness *d* with the bulk refractive index of the disk material, α (see Fig. 2.1).

If, additionally, one takes into account that the dielectric slab has a plane of symmetry then these problems can be reduced to transcendental equations for the even and odd waves of the slab, respectively,

$$\tan(pkd/2) = -\beta^{E,H} gp^{-1},\ \cot(pkd/2) = -\beta^{E,H} gp^{-1}, \qquad (2.11)$$

where $g^2 = (\alpha_{eff}^{E,H})^2 - 1$ and $p^2 = \alpha^2 - (\alpha_{eff}^{E,H})^2$.

The analysis of (2.11) shows that there exists a finite number $Q^{H,E} \geq 1$ of real roots of each equation in (2.11) and $\alpha_{eff\,(q)}^{H,E}$: $1 < \alpha_{eff\,(q)}^{H,E} < \alpha$, ($q = 0,...,Q^{H,E} - 1$). The largest of the roots correspond to the fundamental waves TM_0 and TE_0 that have no cutoff. The even (odd) index of the wave corresponds to the symmetry (anti-symmetry) of the wave field component E_z or H_z relatively to the median plane of the dielectric slab.

Solution of any of (2.11) can be obtained numerically by the Newton method. For the following analysis, it is important to emphasize three conclusions of such analysis. First, the effective refractive index takes a number of discrete values (branches) corresponding to the waves of different symmetry and parity and therefore should be equipped with some indices. Second, all branches besides of the lowest ones, TM_0 and TE_0, have "cutoff", i.e. they appear only if the product *kd* is larger than certain nonzero value. Third, each branch of α_{eff} depends on the frequency (has dispersion) and varies from 1 to α. The curves in Figs. 2.2 and 2.3 demonstrate the dependences of several effective refractive indices on the frequency normalized to the circular disk radius, or on the value of $ka = kd(d/a)^{-1}$.

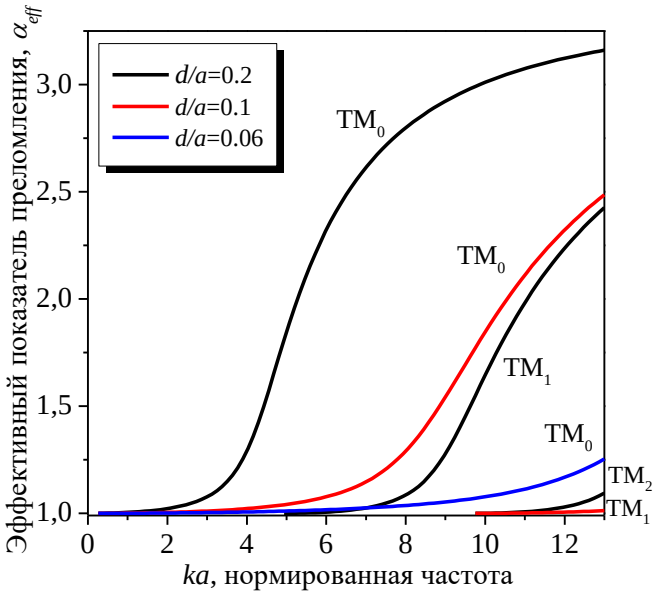

Fig. 2.2 Dispersion curves of the $(E_z)_q$-waves (TM-type) in the dielectric slab made of GaAs. The bulk refractive index is α=3.374

As one can see, the largest of α_{eff} corresponds to the lowest H_z-polarized wave, TE_0. For the disk radii comparable to the free-space wavelength, it is several times greater than the same index corresponding to the lowest E_z-polarized wave, TM_0.

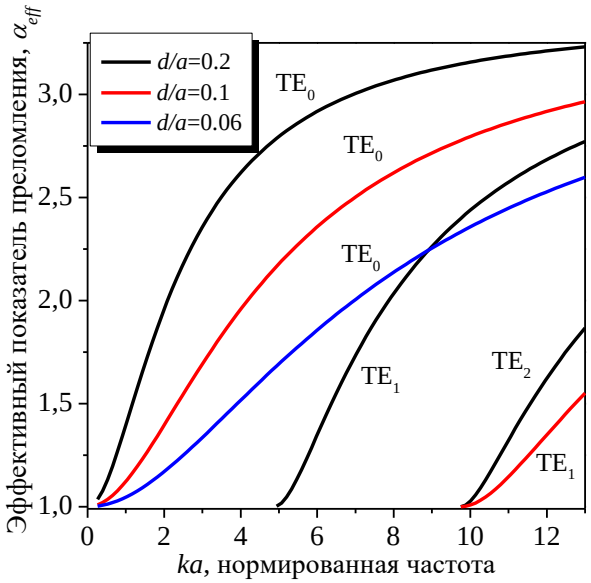

Fig. 2.3 The same as in Fig. 2.2 but for the $(H_z)_q$-waves (TE-type)

Similar situation takes place for the every higher pair of modes of alternative type but of the same indices ($q>1$), however the effective refractive indices of the different-index and different-type waves can be comparable. If the frequency is high enough, then there are many effective refractive indices having the values close to α.

Thus, the reduction of dimensionality of the boundary–value problem for the field in the presence of thin dielectric resonator is an approximate procedure based on the assumption of separability of variables in the resonator plane and in the normal direction. The constant of separation has the meaning, from the one side, of the propagation constant of one of the natural surface waves of the dielectric slab of the same thickness (normalized by the free space wavenumber) in the 1-D *z*-problem, and from the other side, of the effective refractive index in the 2-D in-plane problem.

The effective refractive index happens to be a non-uniquely determined value and strongly depends on the frequency and disk thickness. Its ambiguity and dispersion enable one, in principle, to take account of the finite thickness of resonator (see section 2.3). However, the resonators of optical and microwave filters and couplers, as well as lasers, are usually fabricated thin, with thickness being a fraction of the wavelength. Therefore, when modeling such resonators, the effective refractive index is commonly taken as the largest of all normalized propagation constants, i.e. as that of the lowest (fundamental or principal) H_z-polarized wave, TE_0, whose field does not vary along the *z*–axis and reaches maximum in the center of the slab.

2.2. Formulation of the lasing eigenvalue problem

Before presenting the formulation of the problem for the lasing modes in a resonator with active region, it is reasonable to briefly remind, using the 2-D model, the formulation of the conventional eigenvalue problem for the complex natural frequencies of a passive resonator.

After determining a set of effective refractive indices $\alpha_{eff\,(q)}^{H,E}$ from (2.11), we obtain two independent 2-D problems for the field functions in the plane of disk.

Each of them involves equation (2.8) with piece-constant refractive index and boundary conditions on the contour L of 2-D resonator,

$$U^{-}(r,\varphi)\Big|_L = U^{+}(r,\varphi)\Big|_L, \quad \frac{\partial U^{-}(r,\varphi)}{\partial r}\Big|_L = \beta^{H,E}\frac{\partial U^{+}(r,\varphi)}{\partial r}\Big|_L, \tag{2.12}$$

where the upper index «$\pm$» indicates the limiting values from inside and outside of the contour L, respectively, $\beta^{H} = \left(\alpha^{H}_{eff\,(q)}\right)^{-2}$, and $\beta^{E} = 1$. Besides, the field function has to satisfy the condition of local power finiteness,

$$\int_D \left(|k\,U|^2 + |\,gradU\,|^2\right) r dr d\varphi < \infty, \quad D \subset (r,\varphi), \tag{2.13}$$

and 2-D radiation condition at infinity for the complex values of k. Here one faces the same difficulty as before with the function $V(z)$. In the 3-D case, one can simply take the condition (2.5) with a complex k thanks to the fact that the outgoing fundamental solution to the 3-D Helmholtz equation, e^{ikR}/R, is analytic function of k. In the 2-D case the outgoing fundamental solution is the Hankel function, $H_0^{(1)}(kr)$. However, the domain of analytic continuation of the Hankel function is the infinite-sheet Riemann surface of the function Lnk. Therefore the analog of Sommerfeld condition valid for all complex frequencies k in 2-D has more complicated form known as the Reichardt condition (see [147 – 149]),

$$U(r,\varphi) \sim \sum_{s=-\infty}^{\infty} a_s H_s^{(1)}(kr) e^{is\varphi}, \quad r \to \infty. \tag{2.14}$$

Thus, the equations (2.8), (2.12) - (2.14) form a 2-D complex-frequency eigenvalue problem with effective refractive index $\alpha^{E,H}_{eff\,(q)}$. Note that in order to arrive at this problem, one has to make several assumptions: (i) when imposing condition

(2.9), one has to neglect the finiteness of the disk radius, (ii) when imposing condition (2.12), one has to neglect the finiteness of the disk thickness, and (iii) when imposing conditions (2.10) and (2.14), one has to allow absolutely different field behavior in the disk plane and off that plane (neither of them coinciding with original 3-D spherical-wave behavior). Besides of that, note that (iv) effective refractive index $\alpha_{eff(q)}^{E,H}$ depends on frequency, and (v) it takes discrete set values corresponding to different waves of the associated slab.

Therefore, generally speaking the original 3-D eigenvalue problem is not mathematically equivalent to the «sum" of 1-D and 2-D eigenvalue problems. This is a consequence of the fact that a continuous transformation of 3-D space to the 2-D or 1-D space does not exist. Therefore the dimensionality reduction with the aid of the effective refractive index remains an approximate and non-rigorous technique. Nevertheless, it is well known that the results obtained after using this technique generally agree well with the measurements and frequently have better accuracy than it could be expected [150].

Let us consider now the active cavities. In contrast to the given above formulation, one can modify the eigenvalue problem and look for the real frequencies k [151–152] and non-attenuating in time natural fields, which correspond to the light emission (i.e. to the lasing). To make such fields admissible solutions to the Maxwell equations, one has to introduce new parameter: material gain, $\gamma > 0$, within a certain region inside the open resonator (an active region).

For instance, if the whole volume of dielectric body is filled in with active material, then the active region is bounded by the dielectric resonator boundary, and one has a uniformly active resonator. Suppose that the problem has been already reduced to the 2-D one as explained above and take the refractive index in (2.8) as a complex value, $\nu = \alpha_{eff(q)}^{H,E} - i\gamma$, for $r < a$, and 1 otherwise. At the contour of resonator, let us impose the continuity conditions for the field tangential components, (2.12), with complex ν, i.e. $\beta_{eff}^{H} = \nu^{-2}$ and $\beta_{eff}^{E} = 1$, and request also that condition

(2.13) is satisfied. Eventually, let us request that the Sommerfeld condition of radiation is satisfied at infinity,

$$U(r,\varphi) \sim (2/i\pi kr)^{1/2} e^{ikr} \Phi(\varphi) \qquad r \to \infty, \tag{2.15}$$

Now one can consider equations (2.8), (2.12), (2.13) and (2.15) as a "lasing" eigenvalue problem. This means that instead of the search for the real and imaginary parts of the wavenumber (normalized frequency), as in the conventional eigenvalue problem, one will look for the two positive quantities, k and γ. As the sought frequency *k* is real, the corresponding modal field will not display unlimited growth at infinity in space, as in the conventional (complex-frequency) problem.

He lasing eigenvalue problem can be formulated in the 3-D case as well, as analog to (2.1) – (2.4). Thanks to the well-developed theory of operator-valued functions, the fundamental properties of the eigenvalues in the lasing problem (in the 3-S as well as in the 2-D formulation) can be established before any calculations take place. The proof of these properties can be based on the analytical regularization, i.e. equivalent reduction of the source-free boundary-value problem to the set of Muller boundary integral equations (see Chapter 4), which are the Fredholm second-kind equations [123], and a further use of the operator extensions of the Fredholm theorems [131, 153]. It can be proved that all $\gamma > 0$, and besides that,

- eigenvalues form a discrete set on the (k,γ)-plane,
- eigenvalues do not have finite accumulation points,
- any eigenvalue can have only finite multiplicity,
- eigenvalues may appear or disappear only at the boundaries of the domain of analyticity (at infinity and at the branch points),
- any eigenvalue depends on the shape of contour *L*, resonator thickness *d* and refractive index of the material α in piece-continuous or piece-analytic manner; this dependence can be broken only if two or more eigenvalues coalesce.

2.3. Modes of a uniformly active circular resonator

Geometry of the 3-D model of a thin dielectric disk fully filled in with an active material is shown in Fig. 2.1. Assume that the disk of the thickness *d* and radius *a* is non-magnetic and isotropic and locate din free space. As before, the real part of refractive index will be denoted as α. Suppose also that the electromagnetic field depends on time as $e^{-i\omega t}$ and the free-space wavenumber is $k = \omega / c = 2\pi / \lambda$, where λ is the free-space wavelength. Further assume that the problem has already been reduced to the 2-D one as explained in subsection 2.1. Then either of two polarization states of the field (E and H polarizations) can be considered independently using one function *U*, which is either E_z, or H_z component, i.e. that normal to the disk plane. Strictly speaking, one has to keep in mind that the found from the 2-D model modes are just approximations for the quasi-H_z-polarized or quasi-E_z-polarized modes of thin 3-D disk, because in the real disk still exists a small in magnitude E_z or H_z modal field component, respectively.

The lasing eigenvalue problem (2.8), (2.12)-(2.15) implies that the function *U* must satisfy a 2-D Helmholtz equation (2.8) with a complex refractive index $\nu = \alpha_{eff}^{H,E} - i\gamma$ for $r < a$ and real index $\nu = 1$ in the remaining part of the plane, at $r > a$. In this Chapter, we will assume that the material gain is uniform within the disk, i.e. that γ is a positive constant. The cases of non-uniform gain will be considered in subsection 2.4. At the disk boundary the tangential field components are supposed to be continuous, see (2.12), with coefficients $\beta^H = \nu^{-2}$ or $\beta^E = 1$, depending on polarization. The condition of the local finiteness of energy is given by inequality (2.13), and, in view of real values of *k*, the function *U* must satisfy the 2-D condition of radiation (2.15).

As it has been pointed out to before, when studying a lasing eigenvalue problem we look for two positive numbers, which are here $\kappa = ka$ and γ. The first of them is the lasing frequency, normalized to the disk radius, and the second is the associated material-gain threshold. Here it is important to stress that the threshold

cannot be obtained from the Q-factor (or imaginary part of the frequency, $\mathrm{Im}\,k$) found from the classical eigenvalue problem.

In the considered here case of the circular disk, the contour *L*, of the 2-D model of resonator is the circle of radius *a*. Using the method of separation of variables, we look for the field function as a product,

$$U(r,\varphi) = F(r)\Phi(\varphi) \tag{2.16}$$

of two unknown functions $F(r)$ and $\Phi(\varphi)$.

Substituting this expression into (2.8) and introducing the separation constant *m*, we obtain

$$\frac{d^2F}{dr^2} + \frac{1}{r}\frac{dF}{dr} + \left(\nu^2 r^2 - \frac{m^2}{r}\right)F = 0, \qquad \frac{d^2\Phi}{d\varphi^2} + m^2\Phi = 0, \tag{2.17}$$

where *m*=0,1,2…, and, from (2.16) and (2.17) find the expression for U:

$$U(r,\varphi) = \begin{Bmatrix} AJ_m(\kappa\nu r/a), r<a \\ BH_m^{(1)}(\kappa r/a), r>a \end{Bmatrix} \begin{Bmatrix} \cos \\ \sin \end{Bmatrix} m\varphi, \tag{2.18}$$

where J_m и $H_m^{(1)}$ are the Bessel and Hankel functions, respectively, and *A*, *B* are arbitrary constants.

It should be noted that the field of any natural mode is stationary, i.e. is a standing wave. All modes in the circular resonator split into independent (orthogonal) families according to the azimuth index, *m*, and also according to the symmetry or anti-symmetry with respect to some direction chosen as $\varphi = 0$. Substituting expressions (2.18) with any one of two possible functions of azimuth angle into conditions (2.12), we obtain one and the same complex characteristic equation:

$$F_m(\kappa,\gamma) = 0, \quad m = 0,\pm1,\pm2,\ldots, \tag{2.19}$$

where

$$F_m(\kappa,\gamma) = J_m(\kappa\nu)H_m'^{(1)}(\kappa) - \beta^{E,H}\nu J_m'(\kappa\nu)H_m^{(1)}(\kappa) \qquad (2.20)$$

Thus, the natural modes having $m > 0$ are twice degenerate. The roots of the transcendental set

$$\begin{cases} \mathrm{Re}[F_m(\kappa,\gamma)] = 0, \\ \mathrm{Im}[F_m(\kappa,\gamma)] = 0, \end{cases} \qquad (2.21)$$

generated by the equation (2.19) are the eigenvalues. One can solve this set by a variety of numerical techniques. We have used the secant iterative method [154] in all further computations.

For the numbering of the roots of (2.19) belonging to the same family in the index *m*, another index, *n*, is usually introduced; its value corresponds to the field variations number along the radius.

Consider at first the simplest configuration when the effective refractive index is assumed constant value, i.e. we neglect its dispersion. The results of computations are shown in Figs. 2.4 and 2.5. Cylindrical functions in (2.19) have been computed with machine precision using the direct and inverse recursion [155]. The accuracy of finding the roots by the secant method was maintained at the level of 10^{-8}.

As initial guess at the search for the rots of (2.21), we have been taking the following asymptotic expressions for the normalized frequency of emission valid assuming that α ? 1 (for brevity, here the indices at α are omitted, however one should keep in mind that this value is in fact just one of the possible values of $\alpha_q^{H,E}$, usually for $q = 0$, see section 2.1):

$$\kappa_{mn}^{H,E} \approx \frac{\pi}{2\alpha}\left(m + 2n\,\mathrm{m}\frac{1}{2}\right), \qquad (2.22)$$

and also two different expressions for the threshold values of material gain:

- if $m = \kappa_{mn}^{H,E}$, then the corresponding modes are not of the whispering-gallery type and their thresholds are inverse proportional to the frequency (or index *m*),

$$\gamma_{mn}^{H,E} \approx \frac{\pi}{2\kappa_{mn}^{H,E}} \ln\left(\frac{\alpha+1}{\alpha-1}\right), \tag{2.23}$$

- and if $m \gg \kappa_{mn}^{H,E} \gg m/\alpha$, then the corresponding modes are of the whispering-gallery type and their thresholds exponentially decay with frequency or index *m*,

$$\gamma_{mn}^{H,E} \approx C_{H,E} e^{-2m\ln(2m/\kappa_{mn}^{H,E})} \tag{2.24}$$

where

$$C_E = \frac{e}{4\kappa_{mn}^{E}\alpha}\left(\frac{2m}{e\kappa_{mn}^{E}}\right)^3, \quad C_H = \frac{\alpha\kappa_{mn}^{H} e}{4[m+\left(\kappa_{mn}^{H}\right)^2 + m^2\alpha^2]}\left(\frac{2m}{e\kappa_{mn}^{H}}\right)^3 \tag{2.25}$$

To derive these formulas from (2.19), one should use the asymptotic representations for the cylindrical functions [156].

A study of the published works dealing with the measurements of the light radiated from the thin-disk resonators demonstrates that their working modes are quasi-H_z-polarized [146]. From the expressions (2.22) and (2.24), one can see that the WG-mode thresholds grow up very quickly if the refractive index is increased, as $\gamma_{mn}^{H,E} = O(\alpha^{-2m})$. If, additionally, one takes into account that here $\alpha = \alpha_0^{H,E}$ and, as follows from Fig. 2.2, in a thin disk $\alpha_{eff,0}^{H} \gg \alpha_{eff,0}^{E} \approx 1$, then one can come to the conclusion that the properties of experimentally observed lasing indeed find a good explanation with the aid of the effective refractive index model. This can be viewed as a partial grounding of the mentioned approximate model.

In Figs. 2.4 and 2.5, presented are the results of computations of the natural-mode frequencies and emission thresholds without account of the dispersion of the effective refractive index, for a 200-nm thick disk made of GaAs/InAs. The

wavelength is assumed to be λ=1550 nm. In this case the effective refractive index is $\alpha_{eff} = 2.63$ for the H_z-polarized modes and only $\alpha_{eff} = 1.31$ for the E_z-polarized ones.

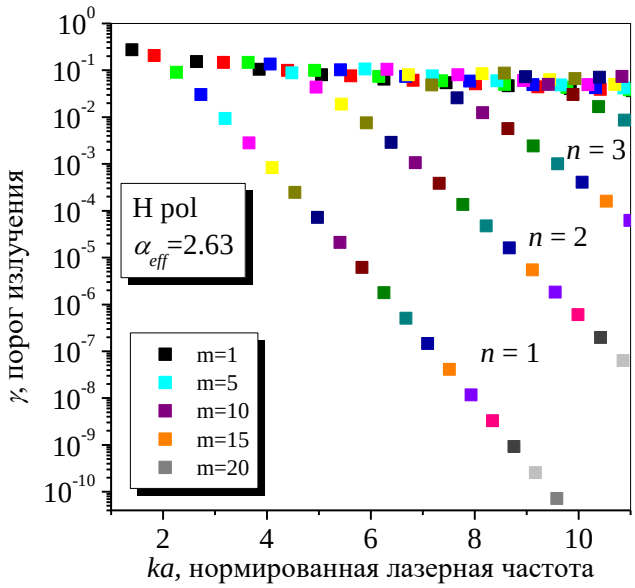

Fig. 2.4 Frequency spectrum and associated thresholds of the H_z-polarized modes H_{mn0} in a GaAs/InAs microdisk, $d = 200$ nm and $\alpha_{eff} = 2.63$ without dispersion.

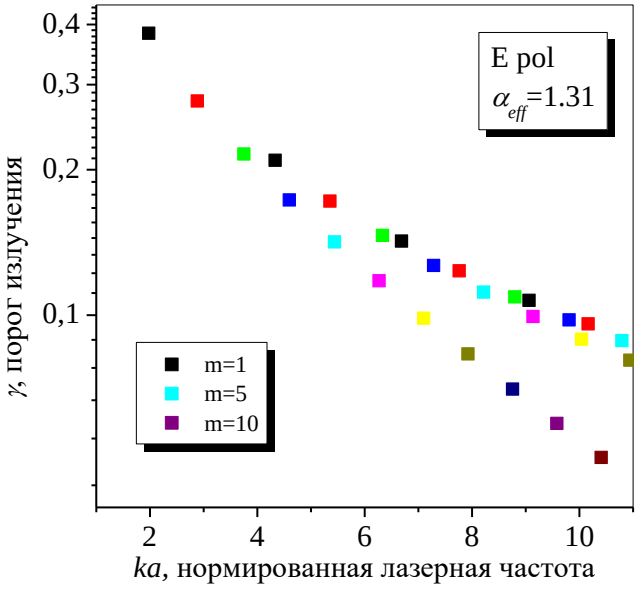

Fig 2.5 The same as in Fig. 2.4 however for the E_z-polarized modes E_{mn0}

Note certain features of the localization of the eigenvalues on the plane (κ,γ). This plane happens to be inhabited by the eigenvalues in non-uniform manner. One can clearly identify the hyperbola $\gamma \approx const/\kappa$, corresponding to the formula (2.23) and "saturated" with the modes of all families in *m*. All these lower-order modes have high thresholds, $\gamma > 0.01$, so that these modes do not display the properties of the whispering-gallery modes. The domain above that hyperbola is free of eigenvalues.

In contrast, in the every modal family having $m > \alpha_{eff}$, the modes whose frequency $\kappa < m$ (approximately $\kappa < m-3$), however still $\kappa > m/\alpha_{eff}$ (approximately $\kappa > m/\alpha_{eff} + 3$), demonstrate very low threshold values of material gain γ. These values are close to those given by the formula (2.24). They go down exponentially (i.e. very quickly) with the growth of the azimuth index *m* in accordance to that asymptotic expression. Therefore below the mentioned hyperbola the eigenvalues form inclined "layers", where each "layer" gathers the modes of a certain radial index *n*. Thus, one can see that the whispering-gallery modes in a 2-D active circular resonator are able to have super-low thresholds characterized by expression (2.24). This is true not only for the modes having the radial $n=1$, but for the higher-order, in radius, modes as well whose fields also experience almost total internal reflection from the disk boundary. However the whispering-gallery modes with single variation along the radius $(n=1)$ form the "elite" of the lasing modes: they form the layer having the lowest thresholds on the plane (κ,γ).

Besides, the comparison of the results presented in Figs. 2.4 and 2.5, demonstrates the effect of the lower effective refractive index value, for the same thin disk, for the E_z-polarized modes than for the H_z-polarized ones. From Fig. 2.5 one can clearly see that in the studied here interval of the frequency variation, $(ka \le 11)$ all eigenvalues of the E_z-polarized modes of a uniformly active circular resonator are located along the hyperbola given by (2.23). The low-threshold whispering-gallery modes of that class have larger frequencies and their calculation need account of the effective refractive index dispersion.

The effective refractive index dispersion can be accurately taken into account if one substitutes this quantity to the characteristic equation (2.19) after finding α_{eff} as one of the roots of corresponding dispersion equation (2.11) computed at the frequency found at the preceding step of the process of computations. A block-diagram of such an adaptive algorithm is presented in Fig. 2.6.

According to the results of subsection 2.1, effective refractive index $\alpha_{eff\,(q)}$ is the normalized propagation constant of the *q*-the surface wave of the flat slab having the same thickness *d* and material as the disk. Therefore the account of the multi-value character of effective index adds the third modal index *q* (integer value) to the notation of the disk eigenmode type (see section 2.1). This corresponds to the approximate description of the possible eigenmode field variations across the real disk, along the *z*–axis. Therefore the roots of (2.19) should be denoted as $(\kappa_{mnq}, \gamma_{mnq})$, where $m, q \geq 0$, $n \geq 1$.

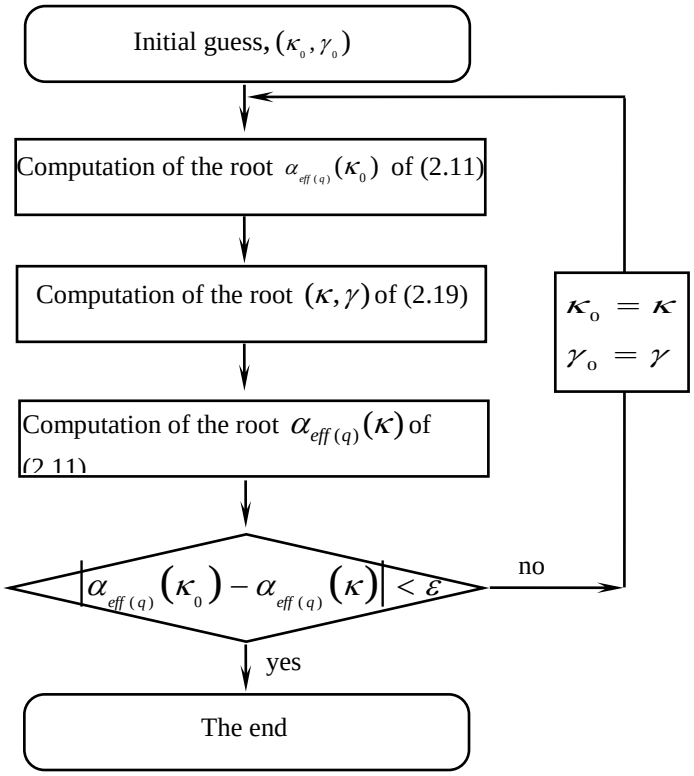

Fig. 2.6 Adaptive computational algorithm

The frequency spectrum and associated thresholds for the modes in the active microdisk laser made of GaAs/InAs having the thickness of $d = 0.1a$, computed with the account of the dispersion of the effective refractive indices connected to the two fundamental waves of the slab, TE_0 and TM_0, are presented in Figs. 2.7 and 2.8, respectively. As one can see, the effect of the effective index dispersion leads to the change of the "angle of inclination" for the eigenvalue layers in comparison to the results presented in Figs. 2.4 and 2.5.

The comparison of the eigenvalues shown in Figs. 2.7 and 2.8 demonstrates the same as revealed without the account of dispersion, namely the effect of much lower effective refractive index associated to the same value of index q for the E_z-polarized modes than for the H_z-polarized ones. This effect is in much higher thresholds of lasing for the E_z-polarized modes than for the H_z-polarized ones. Similar data was obtained for the higher values of effective index associated with $q > 0$. In this case, the eigenvalues shift towards higher values of both frequencies and thresholds that are caused by the lower values of the corresponding refractive indices.

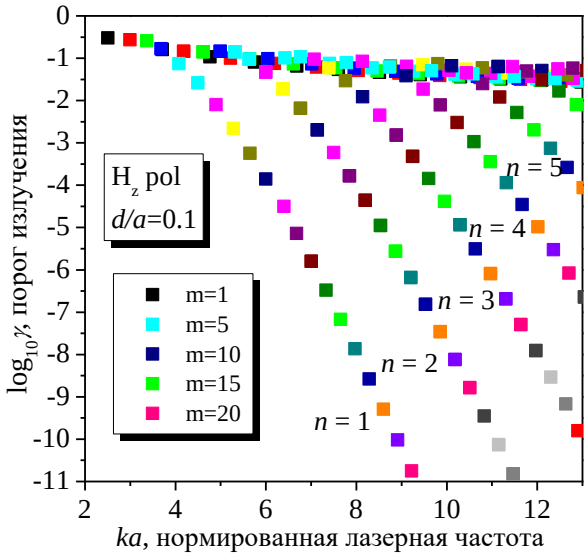

Fig. 2.7 Effect of α_{eff} dispersion on the frequencies and associated thresholds of the H_z-polarized modes H_{mn0} in a GaAs/InAs, $d = 200$ nm, $\alpha = 3.374$ and $d/a = 0.1$

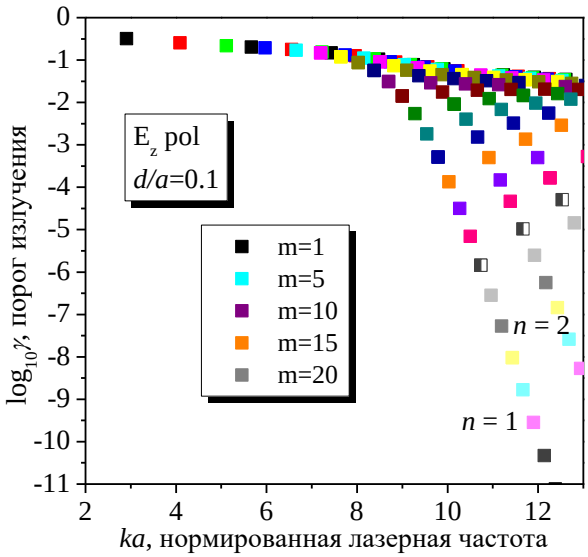

Fig. 2.8 The same as in Fig. 2.7 however for the E_z-polarized modes E_{mn0}

Natural-mode fields of an open active circular resonator have, in the 2-D model, only three non-zero components: one longitudinal of the field corresponding to the polarization, and two transversal, of the alternative field. Neat E-fields of some of the modes in circular resonator are presented in Figs. 2.9 and 2.10.

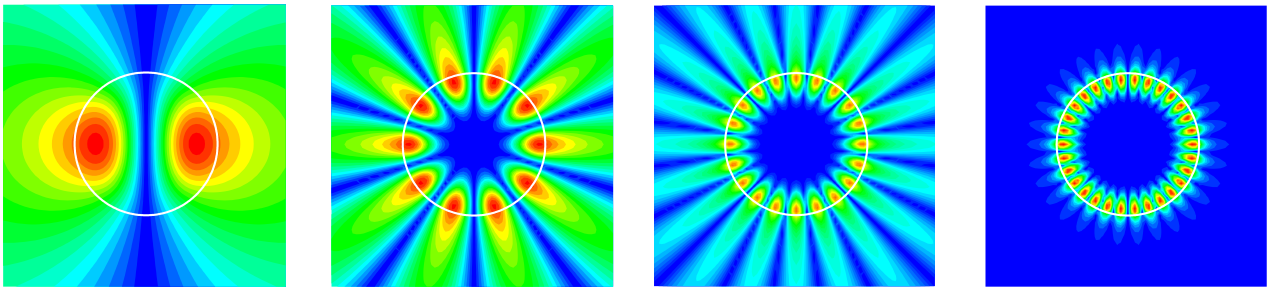

(a) (b) (c) (d)

Fig. 2.9 Near E-fields (absolute value) for the E_z-polarized modes in an active circular microresonator from GaAs, $\alpha = 3.374$ and $d/a = 0.1$: (a) $E_{1,1,0}$, ka=2.9, γ=0.23, α_{eff}=1.01; (b) $E_{5,1,0}$, ka=6.65, γ=0.17, α_{eff}=1.12; (c) $E_{10,1,0}$, ka=8.7, γ=3.1*10^{-2}, α_{eff}=1.46; (d) $E_{15,1,0}$, ka=10.03, γ=1.33*10^{-4}, α_{eff}=1.86

The longitudinal components of the fields age given by expressions (2.18), in which one has to substitute the values of κ and γ found from the characteristic equation (2.19) with corresponding index m. Then the transversal components are found from the Maxwell equations. Frequently when visualizing the fields in 2-D models, researchers build the patterns for the corresponding longitudinal component. However, in practical measurements they always measure the quantities proportional to the square of the absolute value of the electric field; therefore building the patterns in terms of this value is also useful.

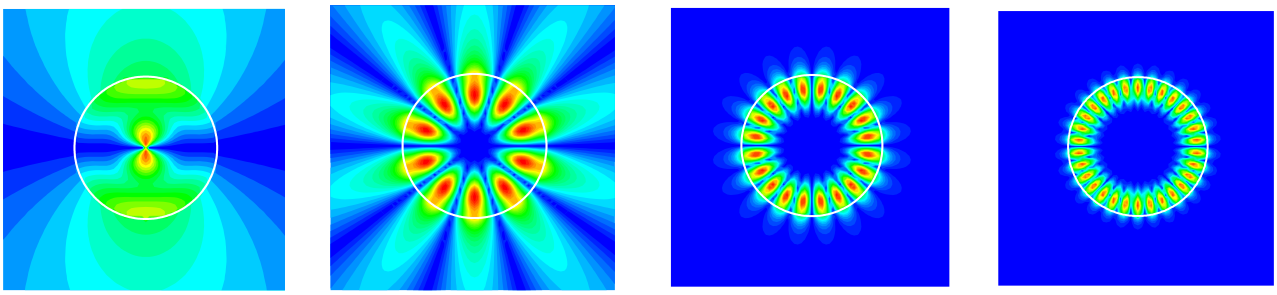

(a) (b) (c) (d)

Fig. 2.10 The same as in Fig. 2.7 however for the H_z-polarized modes: (a) $H_{1,1,0}$, ka=2.5, γ=0.29, α_{eff}=1.55; (b) $H_{5,1,0}$, ka=4.08, γ=7.4*10^{-2}, α_{eff}=1.98; (c) $H_{10,1,0}$, ka=5.99, γ=1.4*10^{-4}, α_{eff}=2.36; (d) $H_{15,1,0}$, ka=7.65, γ=6.8*10^{-8}, α_{eff}=2.58

At any distance from the circular resonator (as well as inside of it) the dependence of the absolute value of the filed, e.g. $|E_z|$ or the power $(|E_r|^2+|E_\varphi|^2)^{1/2}$, on the azimuth coordinate, φ, is given by the function $|\cos m\varphi|$ or $|\sin m\varphi|$. Therefore the modes of the circular resonator radiate $2m$ identical beams or lobes. In general, the near-field patterns show almost total internal reflection of the whispering-gallery mode fields (those with exponentially low thresholds) and intensive leakage of the fields of the lower modes, whose thresholds are high.

To verify the theory, we have compared the obtained results with the experimentally measured spectrum of emission of a microdisk laser made of GaAs

that can be seen in Fig. 2 of the paper [65]. Inside that resonator, there was located an active layer consisting of the InAs quantum dots, and the pumping was arranged in optical way. The measured curve of the photoluminescence intensity is presented at the bottom of Fig. 2.11 where the mode indices are indicated as given by the authors of [65]. Each of the peaks is interpreted as emission of light on the corresponding mode of the disk.

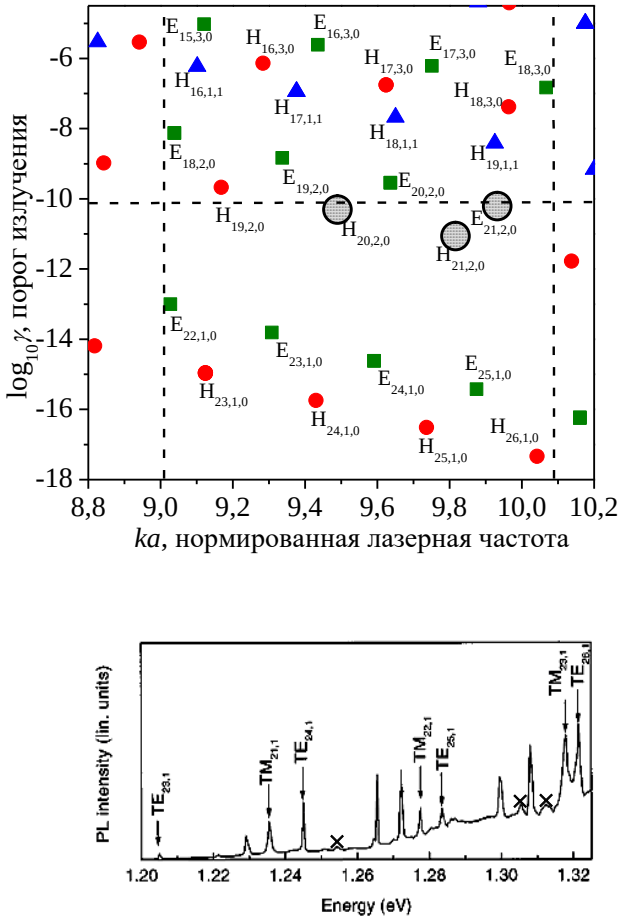

Fig. 2.11 Comparison of the modeling results (top part) and experimental data from [65] (bottom part). The GaAs/InAs disk parameters are α=3.374, radius a=1.5 μm, and thickness d=0.25 μm

The geometrical parameters of the disk fabricated in [65] were as follows: radius 1.5 micron and thickness 250 nm, so that d/a ; 0.17. Such a disk is not

sufficiently thin to restrict the study by considering only the H_z-polarized lasing modes, because two fundamental-mode effective refractive indices are close to each other (see section 1.2).

In the top part of Fig. 2.11, we show the same (bordered with dashed lines) strip of normalized frequencies in the plane (κ, γ), filled in with the lasing eigenvalues computed using our model, for several q values of effective index $\alpha_{eff\,(q)}^{E,H}(\kappa)$. Here, one should be reminded that each eigenvalue is double degenerated.

First of all, note that the peaks on the experimental curve are grouped by pairs (i.e. make doublets) that are explained by the removal of degeneration due to the roughness of the real disk surface. This explanation is fully supported by the observation of the microphotography of the studied microdisk (see Fig. 2.12). It is visible that some indentations on the disk rim are so large that have the dimensions of 20-100 nm. This is the reason of the observed 10-nm splitting of the doublet modes.

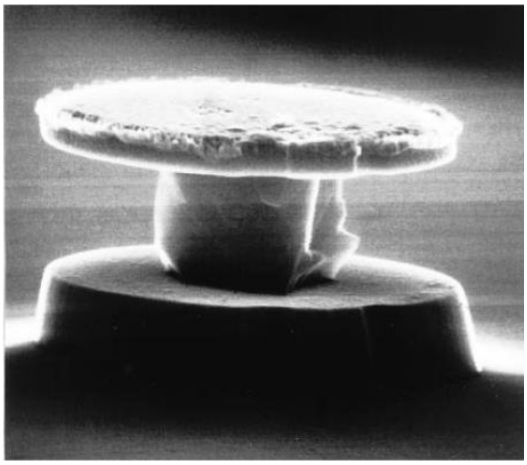

Fig. 2.12 Micro[photography of the 3-micron in diameter microdisk laser whose emission spectrum is shown in the bottom of Fig. 2.11 (borrowed from [65], Fig. 1)

Besides, note that the supporting pedestal is non-symmetric that also leads (on a lesser scale) to the mode degeneracy removal. The comparison of the mode indices shows that the whispering-gallery modes identified in [65] as $TE_{23,1}$ … $TE_{26,1}$, correspond to the doublets from $H_{23,1,0}$ to $H_{26,1,0}$ in our notations and had been almost

correctly identified in [65], although the authors had apparently not realized that in a disk with roughness all modes split to doublets. Still besides, the authors of [65] had correctly established that the alternatively polarized modes, of the *TM* type in their notations, are also emitting light and thus have sufficiently low thresholds of lasing. However, they indicated the peaks corresponding to those modes on the photoluminescence curve as the modes $TM_{21,1}$ … $TM_{23,1}$, while our analysis suggests that they were corresponding to the doublets from $E_{23,1,0}$ to $E_{25,1,0}$.

More detailed study of the experimental curve displays small peaks marked with crosses (×) in Fig. 2.11. Our modeling enables us to suggest that they correspond to the modes having two variations of the field along the radius, namely, $H_{20,2,0}$, $H_{21,2,0}$ and $E_{21,2,0}$, for which the used pumping was just above the thresholds. All other modes whose frequencies lay in the considered band were, apparently, below threshold because the used optical pumping power was not sufficient. The used level of pump power is schematically indicated with a horizontal dashed line in the top of Fig. 2. 11, and the lasing eigenvalues corresponding to the crosses on the experimental curve are marked with circles.

Thus, we can conclude that, first, the 2-D modeling of the disk resonators with the aid of effective refractive index is sufficiently accurate even for the disks with thickness-to-radius ratio as large as 0.2. Second, the proposed here approach to the analysis of the frequencies and thresholds of the lasing modes in the active disk provide the information that agrees well with the experiment.

2.4. Modes of a resonator with the radially inhomogeneous active region

In this section, we consider the lasing eigenvalue problem for the 2-D circular resonator with a radially inhomogeneous material gain. The active region in this case is shaped as either a circle of a smaller radius in the center of resonator, or a ring adjacent to the disk rim. Laser resonators that have active region not coinciding with the whole disk are very interesting objects to be studied with our approach. This is because our model enables one to take account of the active region location in the

resonator and quantify its effect on the frequencies and thresholds of lasing. It should be noted that this situation cannot be studied with the aid of the classical frequency-eigenvalue problem.

Real-life prototypes of the disks with radially inhomogeneous active zones are the microdisk lasers of injection type. These lasers are usually built in such a way that a thin microdisk is sandwiched between a substrate and a metal contact placed on its upper surface. The density of injected carriers (electrons) and hence the material gain has the largest value below the contact and rapidly decays off that area. At the early stage of the development of such lasers, one could see that devices that had the electrode attached to the disk center – see Fig. 1.3. Later on, the lasers having a ring-like contact appeared and now they seem to be common - see Fig. 1.5 (e). Generally speaking, for the improvement of the lasing characteristics of any injection-type laser the shape, size and location of its metal contacts must be designed to match the field in the resonator. These questions are considered in greater details in section 3.4 of this thesis.

When modeling the microcavity injection-type laser shaped as a thin disk, we will assume that the problem has been already reduced to the 2-D one using the method of effective refractive index. Besides, to simplify the analysis we will assume that the material gain, γ , is piece-constant function of the radius only. It means that the gain is either (i) a constant inside the circle of the radius $b < a$ and zero in the ring off that circle, or otherwise, (ii) is zero in the mentioned above inner circle and a constant in the ring adjacent to the disk rim (see Fig. 2.13). Then the refractive index inside the disk is $\nu = \alpha_{eff}$ in its passive part, and $\nu = \alpha_{eff} - i\gamma$ in its active part.

Step-like dependence of the refractive index ν on the radial coordinate leads to the appearance of additional pair of boundary conditions at $r = b$. These conditions are similar to (2.12) valid on the disk boundary, at $r = a$. They consist of the demand of continuity of the tangential components of the mode electromagnetic field. In 2-D problem, they are the continuity of the field function $H_z(E_z)$ across the boundary and of its normal derivative (with the weight $1/\nu^2$ in the case of the H-modes).

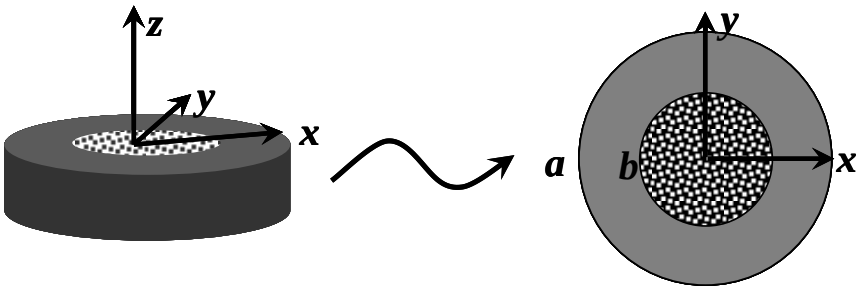

Fig. 2.13 Three-dimensional microdisk laser of injection type and corresponding to it model of reduced dimensionality

Taking account of the conditions of radiation and local power finiteness, the field function in the resonator can be presented in the following form in each of the partial domains:

$$U(r,\varphi)=\begin{Bmatrix} AJ_m(\kappa\nu r/a), r<b \\ BJ_m(\kappa r/a)+CH_m^{(1)}(\kappa\nu r/a), b<r<a \\ DH_m^{(1)}(\kappa r/a), r>a \end{Bmatrix} \begin{Bmatrix} \cos \\ \sin \end{Bmatrix} m\varphi,\ m=0,1,2..., \quad (2.23)$$

where A, B, C, D are arbitrary constants linked by the boundary conditions.

After the substitution of these expressions to the two pairs of the boundary conditions at $r=a$ and $r=b$, one arrives at the following characteristic equation:

$$\det\begin{bmatrix} H_m^{(1)}(\kappa) & -J_m(\kappa\alpha) & -H_m^{(1)}(\kappa\alpha) & 0 \\ H_m'^{(1)}(\kappa) & -\beta\nu J_m'(\kappa\alpha) & -\beta\nu H_m'^{(1)}(\kappa\alpha) & 0 \\ 0 & J_m(\kappa\alpha\delta) & H_m^{(1)}(\kappa\alpha\delta) & -J_m(\kappa\nu\delta) \\ 0 & \beta\nu J_m'(\kappa\alpha\delta) & \beta\nu H_m'^{(1)}(\kappa\alpha\delta) & -J_m'(\kappa\nu\delta) \end{bmatrix}=0, \quad (2.24)$$

where parameter $\delta=b/a$ is the ratio between the radii of the active and passive parts of the resonator.

Numerical results for the frequencies and thresholds of the lasing modes have been computed only for the H_z-polarized modes, in view of their greater importance in thin disks as suggested by the analysis of the effective refractive indices (see

subsection 2.3). In Fig. 2.14, presented are the frequencies and thresholds for the modes of the families $H_{m,n,0}$ in the case of the circular active region located in the disk center and having the radius twice smaller than the disk radius ($\delta = 0.5$). These values have been computed with the account of effective refractive index dispersion.

Comparison of the results in Fig. 2.14 and their counterparts for the microdisk with a uniform gain (Fig. 2.7) shows that, if the active region shrinks in two times (in radius), the modes keep their frequencies however drastically change their thresholds показывает, что при уменьшении активной зоны вдвое (по радиусу) моды. Namely, in a model of the GaAs/InAs disk such a shrinking of the active region results in the 5 to 9 orders of magnitude increment of thresholds of modes whose frequencies are in the interval $ka \le 13$, in comparison to the uniformly active resonator.

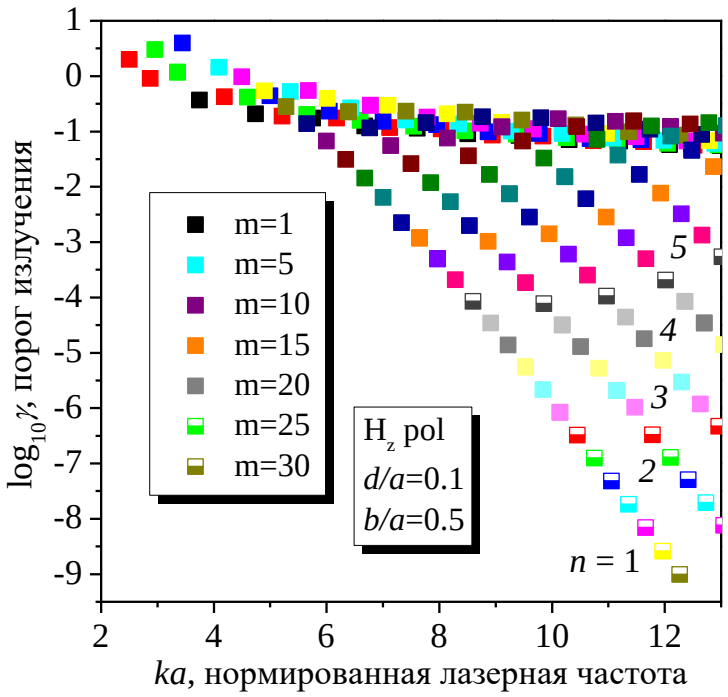

Fig. 2.14 Frequencies and associated thresholds of the H_z-polarized modes H_{mn0} in a GaAs/InAs disk having circular active region of the radius $b = a/2$, $\alpha = 3.374$ and $d/a = 0.1$

To clarify how much and quickly thresholds grow up, we have studied the dependences of the eigenvalues on the relative radius of the active region. In Fig. 2.15, the dashed lines show the thresholds of three whispering-gallery modes $H_{m,1,0}$ (m = 5,10,15) as a function of the parameter δ that is the ratio of the central active region radius to the disk radius. One can see that even small reduction of the active region, in this configuration, plays extremely destructive role.

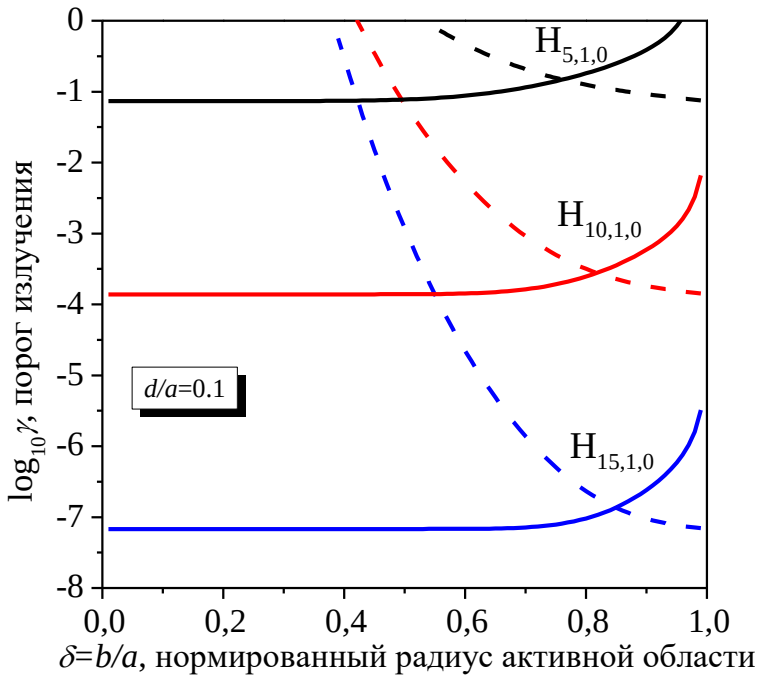

Fig. 2.15 dependences of the thresholds of the whispering-gallery modes of the family $H_{m,1,0}$ in a GaAs/InAs disk on the relative radius of the active region. Solid curves are for the case of ring-like active region and the dashed curves are for the circular active region in the disk center; $\alpha = 3.374$ and $d/a = 0.1$

As already mentioned, the alternative configuration with radially inhomogeneous active region is realized with the aid of a ring-like contact for the injection of carriers into the area around the disk rim. Note that the same configuration of active region can be achieved by using the optical pumping of the disk with embedded quantum wells or layers of quantum dots. Here, one has to

transfer the pumping beam through an axicon to make it hollow with a dark spot in the center [157].

For a circular resonator having a circular-ring active region, we derive the characteristic equation that looks like (2.23) but with the values ν and α exchanged their places. The computation of its roots, or pairs of numbers (κ,γ), shows that the thresholds of the whispering-gallery modes keep the same values as in the uniformly active disk even is the ring width is only a fraction of the whole disk radius.

The corresponding dependences of thresholds on the relative inner radius of the active region δ are also presented in Fig. 2.15, by the solid lines. Note that these dependences have been computed with full account of the effective refractive index dispersion. The thresholds grow up monotonically with the narrowing of the active ring; however a noticeable change starts only when the active region becomes narrower than the area occupied with the bright spots of the field. As these spots are more concentrated at the resonator rim for the modes having larger azimuth indices *m* (see Fig. 2.10), the active region for such modes can be made very narrow without a damaging effect on the emission thresholds.

It is interesting to note that the crossing of the solid and dashed curves in Fig. 2.15 for the modes of the same type takes place at the level of exactly twice larger (within the accuracy of several digits) threshold than for a uniformly active disk. This effect will be explained in section 3.4.

Thus, creation of an active region in the disk center, as in the injection-type lasers with centrally located electrode, has catastrophic action on the ultra-low thresholds typical for the whispering-gallery modes in a circular resonator. In the opposite case, when active region is arranged as a ring along the disk rim, the thresholds keep their ultra-low values. This enables one to reduce significantly (proportionally to the ratio of the whole disk area to the ring area) the power of pumping or, respectively, the output power of laser [157, 158].

CONCLUSIONS FOR CHAPTER 2

In this Chapter, we have considered the general questions related to the correct formulation of the lasing eigenvalue problem for the open dielectric resonators with active regions. Further the modes of several simple configurations of circular-cavity lasers with uniform and non-uniform gain have been studied numerically and analytically. The results of this study that have been published in journals [1, 2] and conference proceedings [9-10, 12-14] enable us to make the following conclusions:

1. If an open dielectric resonator is shaped as a thin "disk" with arbitrary contour of the side surface, then the dimensionality of the corresponding electromagnetic problem can be approximately reduced from 3-D to 2-D, in the disk plane. Instead of the bulk refractive index, in the reduced-dimensionality problem one has to use the "effective refractive index," which is generally a multi-valued function of the disk thickness, its bulk refractive index, and the wavelength.

2. Introduction, into the model of open resonator, of the active region whose material possesses non-zero imaginary part of refractive index (or effective refractive index) with appropriate sign (corresponding to the "negative losses") leads to new electromagnetic eigenvalue problem. Such a problem enables one to determine the frequencies and the associated thresholds of emission for the natural modes of the active resonator.

3. The spectrum of the natural lasing modes of an open resonator with active region has discrete character and each mode has its own specific value of material threshold given by the imaginary part of the refractive index of active material. The frequencies and the thresholds of each mode continuously depend on the other parameters.

4. The natural lasing modes of the uniformly active 2-D circular resonator display different types of behavior depending on the value of the azimuth index, m. Lower-index modes are strongly leaky and have high thresholds, which are inverse

proportional to the emission frequency. In contrast, higher-index modes show the properties of the whispering gallery (their fields are weakly leaky and are contracted to the resonator's rim from inside) and their thresholds are exponentially low with respect to the emission frequency or the mode azimuth index.

5. If the active region in a circular resonator is shaped as a circular region of a smaller radius in its center, then the thresholds of the whispering-gallery modes take catastrophically larger values than in the uniformly active resonator.

6. If the active region in a circular resonator is shaped as a ring adjacent to the resonator rim, then the thresholds of the whispering-gallery modes keep their ultra-low values even if the mentioned active ring is narrow and its width is a small fraction of the resonator radius.